JOURNAL OF MATERIALS SCIENCE 21 (1986) 2926–2932

Electrical conductivity study of oxidation process in manganese-substituted magnetites

B. GILLOT, M. EL GUENDOUZI
Laboratoire de Recherches sur la Réactivité des Solides UA 23, Faculté des Sciences Mirande, BP 138, 21004 Dijon Cedex, France

A. ROUSSET, P. TAILHADES
Laboratoire de Chimie des Matériaux Inorganiques, Université Paul Sabatier, Toulouse III, 118 route de Narbonne, 3100 Toulouse, France

During oxidation in air of finely-grained manganese-substituted magnetites $(Mn^{2+}_{0.8x}Fe^{3+}_{1-0.8x})_A$-$(Fe^{3+}_{1+0.6x}Fe^{2+}_{1-0.8x}Mn^{3+}_{0.2x})_BO^{2-}_4$ (A = tetrahedral, B = octahedral) the temperature dependence of the electrical conductivity over a temperature range of 100 to 700° C was investigated. Below 500° C the evolution of electrical conductivity might be closely associated with the position and nature of cations in the spinel lattice. The profile of the $\sigma = f(t)$ curves show that the mechanism of electrical conduction in the temperature range 150 to 300° C can be explained in terms of the oxidation of Fe^{2+} to Fe^{3+} ions at octahedral sites. For the temperature range 300 to 400° C the conductivity involves the hopping of electrons from tetrahedral-site Mn^{2+} ions to tetrahedral-site Mn^{3+} ions. Above 500° C the oxidation of Mn^{2+} ions leads to an increase in conductivity with the generation of new phases of α-Fe_2O_3, Mn_2O_3 and α-$(MnFe)_2O_3$.

1. Introduction

Recent studies have been devoted to the electrical properties of several fine-grained magnetites of type $(Fe_{3-x}M_x)O_4$ substituted by trivalent ($M = Al^{3+}$, Cr^{3+}) or divalent ($M = Co^{2+}$, Zn^{2+}) ions and to the evolution of this conductivity in the presence of oxygen during the formation of metastable γ defect phases [1, 2] and their transformation to rhombohedral α phases [3]. These phases are obtained only by the oxidation of Fe^{2+} ions where the degree of oxidation z is defined by the relation

$$Fe^{2+} + \tfrac{1}{2}zO \rightarrow zFe^{3+} + (1 - z)Fe^{2+} + \tfrac{1}{2}zO_2^-$$

in the process of low-temperature oxidation ($T <$ 400° C) with maintainance of the spinel structure, the conduction mechanism can be envisaged as an electron hopping between Fe^{2+} and Fe^{3+} ions, $Fe^{3+} \rightleftarrows (Fe^{2+} + e)$, and this valence transfer may occur at octahedral sites (B sites) as well as tetrahedral sites (A sites). Inverse spinels such as magnetite, with a high initial conductivity and which are n-type semiconductors, undergo a large conductivity decrease during oxidation related to the generation of Fe^{3+} ions and vacancies at B sites upsetting the electron exchange between the Fe^{2+} and Fe^{3+} ions initially present in equal amounts at B sites. This possibility of "hopping" between Fe^{2+} and Fe^{3+} ions has also been observed at tetrahedral sites during the oxidation of normal spinels, which initially only contain Fe^{2+} ions at these sites. Thus, when Fe^{3+} ions prevail, the conductivity decreases as for inverse spinel until the γ compound is obtained. Moreover, above about 400° C, these metastable γ defect phases gradually transform into rhombohedral α phases of the same bulk composition, and the electrical conductivity yields discontinuities and a change in plots of $\log \sigma$ against $f(1/T)$ [3].

The situation is different for manganese-substituted magnetites in which two cations are likely to be oxidized (Fe^{2+} and Mn^{2+}) at relatively low temperature, and where the transformation mechanism is more complicated than in the case of the $\gamma \rightarrow \alpha$-$Fe_2O_3 + MFe_2O_4$ or $\gamma \rightarrow \alpha$-$Fe_{6-y}M_yO_9$ transformation [4] because of the presence of manganese ions leading to oxidation–reduction phenomena. During a study of the oxidation of these spinels by thermogravimetry [5] it was found that the availability for oxidation of Mn^{2+} ions in A sites is much less than for Fe^{2+} and Mn^{3+} ions in B sites, and that above about 550° C the γ defect phases are oxidized with a phase change from the spinel structure into the corundum structure.

In this paper an attempt has been made to use another structurally sensitive physical parameter, electrical conductivity, to characterize the process of oxidation at temperatures up to 700° C, and provide an interpretation of the thermogravimetric data in terms of the distribution of ions of manganese and iron. In addition, during the treatment in oxygen some of these ions promote a partial oxidation or reduction. As a consequence of this action, they may introduce a certain number of ions of different valency in the lattice, and quite small quantities of such ions can result in a relatively large change in conductivity.

2. Samples and experimental methods

2.1. Samples

The preparation conditions of finely-grained manganese-substituted magnetites do not differ from the method previously used to prepare M^{3+}- or M^{2+}-

0022–2461/86 $03.00 + .12

TABLE I Sample characteristics

Sample $Fe_{3-x}Mn_xO_4$ x	Lattice parameter (nm)	Specific area ($m^2 g^{-1}$)	Particle size (nm)
0.14	0.8412	22	54
0.27	0.8428	23	51
0.37	0.8437	25	45
0.50	0.8457	21	59
0.72	0.8473	20	63
0.93	0.8490	24	48
0.97	0.8494	17	71

substituted magnetites [6]. The thermal decomposition of mixed oxalates of iron and manganese such as $(Fe_{1-x}Mn_x)C_2O_4 \cdot 2H_2O$ $(0 < x < 1/3)$ leads, through adequate thermal treatments at low temperature ($< 500°$ C) to the solid solutions $(Fe_3O_4)_{1-x}$-$(MnFe_2O_4)_x$, which are extremely divided solids and hence largely reactive.

Radiocrystallographic analysis at room temperature performed with diagrams obtained in vacuum with monochromatized Cr$K\alpha$ radiation shows that the samples contain only the spinel phase with the totality of Mn^{2+} ions on A sites and a small amount of Mn^{3+} ions on B sites, resulting in the structural formula

$$(Mn^{2+}_{0.8x}Fe^{3+}_{1-0.8x})_A(Fe^{3+}_{1+0.6x}Fe^{2+}_{1-0.8x}Mn^{3+}_{0.2x})_B O^{2-}_4$$

The lattice parameter increasing approximately linearly with the extent of substitution, x (Table I) and the distribution agrees reasonably well with the neutron diffraction work of Hastings and Corliss [7] indicating that $MnFe_2O_4$ is a normal spinel.

The particle size of samples prepared at 500° C is less than 100 nm (Table I). Moreover, the particle mean diameter deduced from specific surface area measurement is in a good accordance with that obtained by means of electron microscopy and X-ray line broadening.

2.2. Measurements

The d.c. conductivity was measured by means of a two-probe method on compressed sintered pellets of about 0.8 cm diameter and 0.2 cm thickness as reported by Gillot and Ferriot [8]. Care was taken to minimize contact resistance. In this study no attempt was made to determine accurately the absolute value of the conductivity, since it was the temperature variation of conductivity that was of interest. The samples were oxidized isothermally in the conductivity apparatus, or the temperature was increased at a linear rate from room temperature to 700° C. Before each experiment great care had to be taken during heat treatment in the cell (850° C for 1 h in a vacuum of $< 10^{-4}$ Pa) to ensure that the powder was not even partially oxidized. The intermediate phases present after oxidation were determined by X-ray powder diffraction from samples rapidly cooled from various temperature in the cell.

3. Results and discussion

3.1. Behaviour of manganese-substituted magnetites in air

The effect of temperautre on the oxidation characteristics was demonstrated directly by observing the different thermal analysis (DTA) curve and the plots of log σ when samples of different composition were heated in air (Fig. 1). In Region I, the electrical conductivity decreases with increase in temperature and is accompanied by an exothermic DTA peak. This decrease is due to the oxidation of Fe^{2+} ions and consequently to a decrease of Fe^{2+}–Fe^{3+} pairs because the vacancies created do not contribute to the conductivity. Such decreases of conductivity and DTA peak have also been found in other substituted magnetites having initially Fe^{2+} on B sites [2]. The decrease in σ is then followed by an increase in σ corresponding to complete oxidation to γ (hatched Region II). Whatever the value of x, this evolution is not roughly linear as in the case of cobalt-substituted magnetite in which only one cation is oxidized. In addition, a second exothermic DTA peak is also seen in Region II (Fig. 1) and the thermogravimetric (TG) curves indicate a continuous weight gain. In addition, the maximum in Region II (Point A) is shifted toward lower temperatures with increased manganese substitution. The presence of Mn^{2+} ions is probably responsible for this behaviour, and the deviation from linearity in log $\sigma = f(T)$ curves could be due to the oxidation of Mn^{2+} ions in A sites. After oxidation of the compound heated to about 450° C, X-ray analysis should show a single phase of spinel structure with only a decrease of lattice parameter. Thus conduction is likely to take place by the hopping of electrons between Mn^{2+} and Mn^{3+} ions at A sites, which is however less favourable than for B sites since the distances A–A in the spinels are longer than the distances B–B.

At higher temperatures the log $\sigma = f(T)$ curves show a non-linear conductivity in which two or three breaks can be distinguished (Regions III, IV and V, Fig. 1). IN Region III, DTA gives a small endothermic peak at about 470° C corresponding to a partial reduction of manganese ions, but the spinel structure was always maintained. Between 480 and 600° C, a steep increase in σ is observed (represented by dashed lines in Region IV) and there is also in this temperature range an exothermic DTA peak. During an examination of the powder diffraction pattern of the sample heated to 600° C a large number of lines was observed in contrast to the few lines of the spinel structure. Some of the lines can be identified with those of orthorhombic Mn_2O_3 and α-Fe_2O_3. Thus in the temperature range corresponding to Region IV, the steep increase in σ can be regarded as being caused by a phase change from a spinel structure to a corundum structure. It should be noted here that the oxidation of Mn^{2+} ions which are not totally oxidized at lower temperatures (as indicated by the weight gain from thermogravimetric analysis [5]) can contribute to this increase in σ. If we represent the starting and finishing temperatures of the transformation by T_D and T_E, respectively, it was found that a significant shift of T_D and T_E toward higher temperatures was observed with an increase in substitution (Fig. 1). The relationships between T_D, T_E, $T_M = (T_D + T_E)/2$ and the extent of substitution are given in Table II.

Since all the information on temperature dependence is essentially divided into regions, it is convenient for

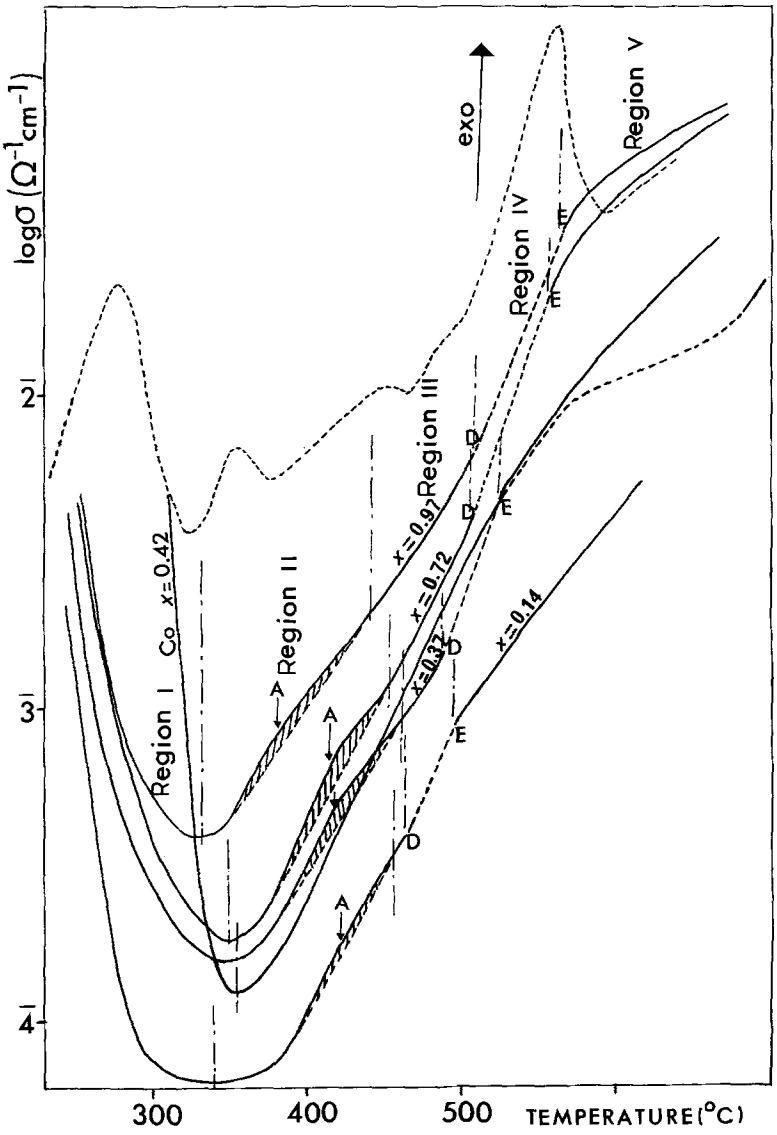

Figure 1 Behaviour of electrical conductivity in air of manganese-substituted magnetites, and DTA peaks (upper dashed curve).

the purpose of this study to examine it separately from the Fe–Mn compositional dependence, which can be adequately represented under isothermal conditions.

3.2. Evolution of electrical conductivity with time during the oxidation process

3.2.1. Oxidation kinetics in Region I

Oxygen at a pressure of 3.3×10^3 Pa was introduced into the cell and the conductivity σ_t at different intervals of time was noted. From the results presented in Fig. 2 for two selected compositions, it can be seen that the conductivity σ_t decreases and that this conductivity depends on the amount of Fe^{2+} ions. The decrease $\Delta\sigma$ (Fig. 2) is larger at lower substitutions than that for higher values of x, acording to the amount of Fe^{2+} ions initially present. According to the model of valence transfer, the decrease in σ_t sensitively reflects the effect of the degree of oxidation z, i.e. with increasing non-stoichiometry the electrical conductivity decreases markedly. This can be explained by a decrease of Fe^{2+} ions with increasing value of the number of vacancies, and consequently a decrease of Fe^{2+}–Fe^{3+} pairs, because the vacancies created do not contribute to the conductivity. At this stage, when all the octahedral Fe^{2+} ions have been oxidized, the distribution in the partial oxidation product will be governed by the initial cation distribution and the vacancies will occur largely on octahedral sites according to the formula

$$(MN^{2+}_{0.8x}Fe^{3+}_{1-0.8x})_A(Fe^{3+}_{(5+0.2x)/3}\square_{Fe^{2+}(1-0.8x)/3}Mn^{3+}_{0.2x})_BO^{2-}_4$$

where □ denotes vacancies. The presence of a small amount of Mn^{3+} ions which prefer octahedral positions does not appear to play a role in the mechanism of conduction, although in the temperature range 250 to 350° C some Mn^{3+} ions will be partially oxidized to Mn^{4+} ions as indicated from the DTG curves [5]. Therefore, if all the Mn^{3+} ions initially in the sample are converted to Mn^{4+} ions (probably above 300° C)

TABLE II Evolution of the transformation temperature

Sample x	T_D (° C)	T_E (° C)	$(T_D + T_E)/2 = T_M$ (° C)
0.14	482	498	490
0.27	491	509	500
0.37	492	528	510
0.50	504	536	520
0.72	504	548	526
0.93	514	558	536
0.97	508	562	540

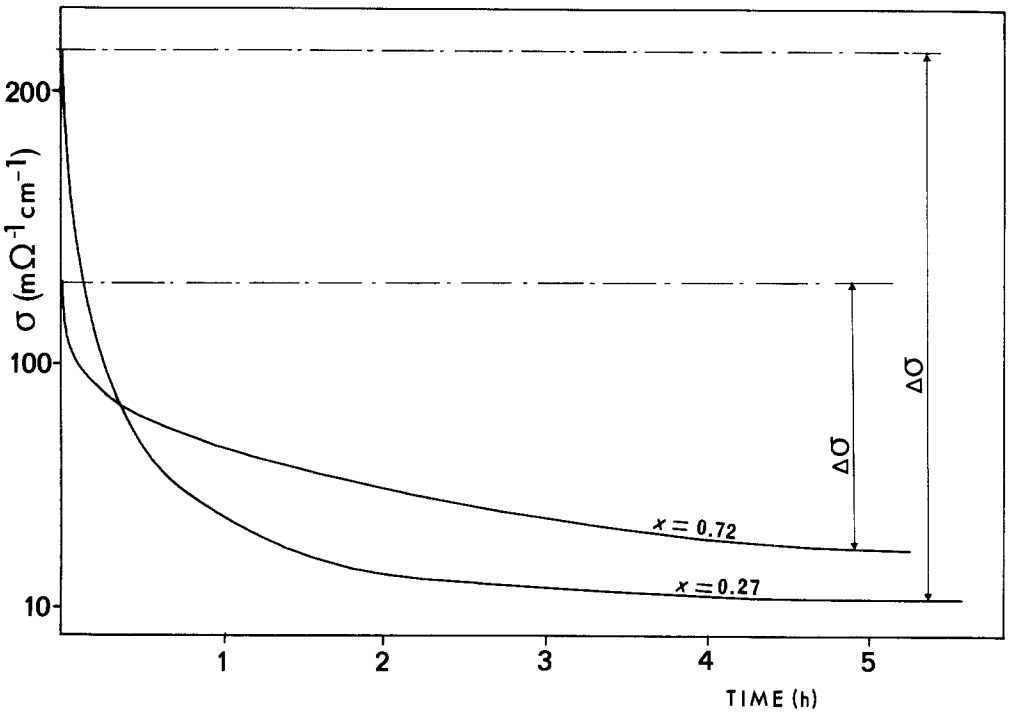

Figure 2 Oxidation isotherms of Fe^{2+} ions in Region I. $T = 175°C$.

the structural formula can be written as

$$(Mn^{2+}_{0.8x}Fe^{3+}_{1-0.8x})_A(Fe^{3+}_{(5+0.2x)/3}\square_{Fe^{2+}(1-0.8x)/3}Mn^{4+}_{(0.3x)/2}\cdots \square_{Mn^{3+}(0.2x)/4})_B O_4^{2-}$$

For the composition $x = 0.50$, we have also plotted the $a = f(t)$ curves, α being the degree of transformation defined by $\alpha = (\sigma_0 - \sigma_t)/(\sigma_0 - \sigma_f)$, where σ_0 = initial conductivity in vacuum, σ_t = conductivity in oxygen at time t and σ_f = final conductivity. Such curves are reported in Fig. 3. The reaction was characterized by a rapid initial stage, declining regularly according to a parabolic law, suggestive of a typical diffusion-controlled process [9] with the production of cation-deficient spinel. This behaviour in the presence of oxygen is similar to that already observed for magnetites slightly substituted with aluminium or chromium in which all Fe^{2+} ions are also on octahedral sites.

3.2.2. Oxidation kinetics in Region II

After oxidation of samples in air at about 320° C, the gas was pumped out at the end of a run, the temperature was raised to Region II and oxygen was admitted at a known pressure. In all cases, the conductivity decreases initially against time, then increases and finally remains practically constant until the γ compound is obtained (Fig. 4). For comparison we have reported the conductivity variation for a cobalt-substituted magnetite previously oxidized at 320° C. In contrast to manganese-substituted magnetites, σ is independent of time and the relatively long plateau of nearly constant conductivity indicates the stability of the γ phase in the presence of oxygen.

The discrepancy of reactivity between Fe^{2+} ions located at B sites and Mn^{2+} ions located at A sites can explain the time dependence of electrical conductivity. A decrease in the conductivity at the onset seems to point to the fact that some Fe^{2+} ions remains

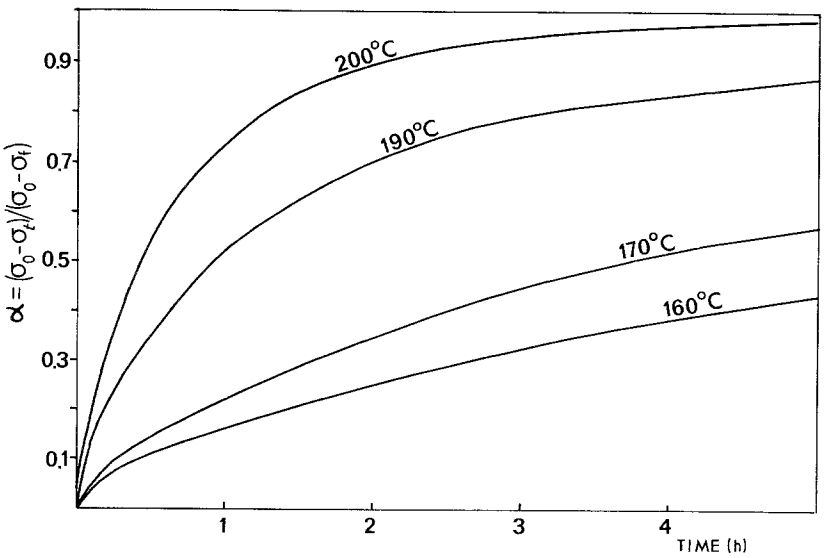

Figure 3 $\alpha = f(t)$ curves for composition $x = 0.50$.

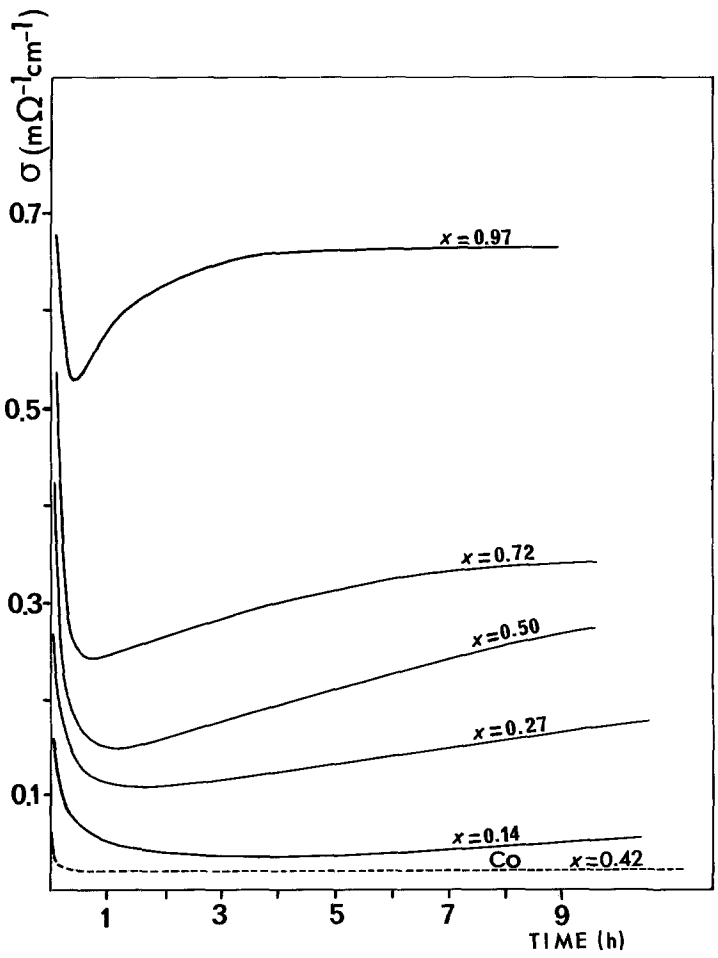

Figure 4 Oxidation isotherms of Mn^{2+} ions in Region II. $T = 360°C$.

unoxidized at the lower temperature, becoming oxidized in the higher temperature range. Moreover, some Fe^{3+} ions must be reduced to lower valency before the admittance of oxygen in the cell, and this would suffice to give primarily a semiconducting behaviour. When all the octahedral Fe^{2+} and Mn^{3+} ions have been oxidized, the reaction can only proceed by the oxidation of tetrahedral Mn^{2+} ions.

After the minimum, the presence of Mn^{3+} ions at A sites appears to provide an explanation for the fact that the conductivity increases, since this can be associated with mixed valencies at A sites. The conductivity is then a result of the transfer of electrons from A-site Mn^{2+} ions to A-site Mn^{3+} ions. It can be observed that, as can be expected, higher Mn^{2+} concentration leads to a more important increase of conductivity. Comparison may be made with the result for chromium- or aluminium-substituted magnetites [1] where all Fe^{2+} ions are at tetrahedral sites and whose increase of conductivity during oxidation can also be explained by the existence of a transfer of electron from A-site Fe^{2+} ions to A-site Fe^{3+} ions. In this case a maximum of conductivity occurs approximately when the amounts of Fe^{2+} and Fe^{3+} ions at A sites are equivalent. Then, when the amount of Fe^{3+} ions becomes large, the electronic exchange is upset and the conductivity decreases. In manganese-substituted magnetites, the time-dependence of the electrical conductivity can be explained on the basis of this mechanism.

However, as confirmed by thermogravimetric investigation, Mn^{2+} ions were not completely oxidized. The results show that the degree of oxidation δ of Mn^{2+} ions reaches the value of $0.8x$ [5] at $T = 400°C$ and $P_{O_2} = 2 \times 10^4$ Pa. The number of vacancies produced in this way in Position A will therefore be limited as a result of the partial oxidation of Mn^{2+} ions. A calculation of the cation distribution in A sites using the δ value of $0.8x$ reveals that the presence of Mn^{2+} ions can contribute to a higher conductivity according to the ionic distribution at tetrahedral sites:

$$[(1 - \delta)Mn^{2+}_{0.8x}\delta Mn^{3+}_{(1.6x)/3}Fe^{3+}_{1-0.8x}\square_{Mn^{2+}(0.8x\delta)/3}]_A$$

If we consider this possibility and the fact that $\delta = 0.8x$, for $x = 0.97$ the formula becomes

$$(Mn^{2+}_{0.174}Mn^{3+}_{0.403}Fe^{3+}_{0.224}\square_{Mn^{2+}0.2})_A$$

In Region II, the conduction can then take place by electron exchange between the manganese ions during a long oxidation time. Another point to notice is that probably, as in some similar cases [10], all vacancies massively migrate from the tetrahedral into the octahedral sublattice, favouring the electron exchange process.

3.2.3. Influence of oxygen pressure on oxidation–reduction phenomena in Region III

In Region III, the effect of oxygen pressure on the oxidation–reduction phenomena has been demonstrated directly by observing the weight loss when the oxygen pressure is decreasing, especially when it is much lower than in air. Based on this loss in weight and from X-ray analysis, the reaction corresponds to

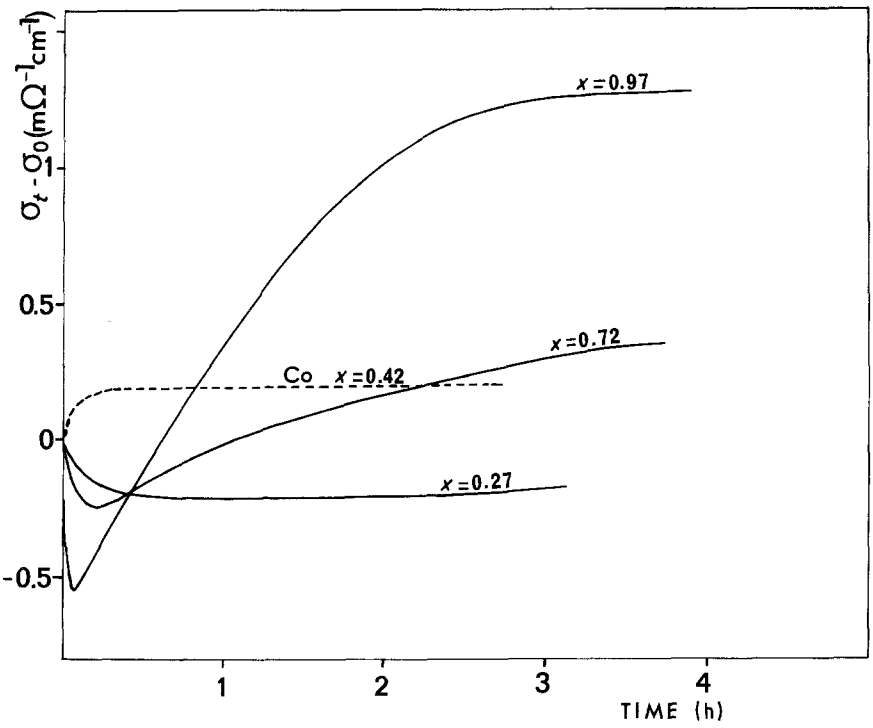

Figure 5 Reduction isotherms in Region III. $T = 455°C$.

the reduction of Mn^{4+} to Mn^{3+} ions at octahedral sites [5]. These Mn^{4+} ions have been created during the oxidation process in Region II.

In order to analyse the effect of this reduction, conductivity measurements were carried out on samples previously heated in air at 455° C and then exposed to low oxygen pressure (13.3 Pa). The change in conductivity is given by $\Delta\sigma = \sigma_t - \sigma_0$ where σ_0 = initial conductivity in air and σ_t = conductivity at time t. It can be seen from Fig. 5 that after an initial period of short duration the conductivity increases, according with an electron exchange between Mn^{3+} and Mn^{4+} ions at octahedral sites. $\Delta\sigma$ also reflects the compositional dependence. If the extent of manganese substitution x is slight or zero (cobalt-substituted magnetite) $\Delta\sigma$ is independent of time and, if the extent of manganese-substitution is high, the oxidation effect is important.

3.2.4. Oxidation process in Region IV

As mentioned above, the transformation from γ defect phases to corundum structure can be directly investigated by evaluating the behaviour of the electrical conductivity in Region IV. However, this phase change is accomplished by oxidation of Mn^{2+} ions. The kinetics of transformation were studied for $P_{O_2} = 2 \times 10^4$ Pa by heating at constant temperature and observing the change in conductivity with time. Fig. 6 shows the kinetic curves during oxidation against composition, x. These curves display a two-stage oxidation process. The initial pattern is a smooth parabolic curve where the oxidized amount (shown by an arrow in Fig. 6) is due to the experimental procedure and increases with the extent of substitution x. Briefly, the procedure was as follows: after oxidation of the sample at about 400° C, the gas was pumped out at the end of a run, the temperature was raised to the transformation temperature (600° C) and oxygen was admitted at a known pressure but lower than its partial pressure in air. Thus, samples heated in this cycle and brought to the final temperature of 600° C were partially reduced in vacuum or at a low oxygen pressure. As a result of this thermal treatment, a certain part of the manganese ions must be reduced with lower valency, i.e. as Mn^{2+} ions. We have also before oxidation two different Mn^{2+} ions: Mn^{2+} ions created by reduction whose amount depends on the thermal treatment, and Mn^{2+} ions not completely oxidized at 400° C. The parabolic curves corresponds to oxidation of Mn^{2+} ions generate by reduction, and the phase may be considered as having a spinel structure as confirmed by X-ray diffraction. This reduction can be eliminated (as can the parabolic stage) if the temperature is raised to the transformation temperature while the oxygen pressure is maintained at 10^2 Pa or higher.

For the second stage corresponding to Mn^{2+} ions not totally oxidized, the σ–t plots are linear and then reach a steady state which represents the state of complete oxidation. For the linear portion corresponding to a phase change this method is not reliable as a measure of the weight change [5] because in this region the electrical conductivity at the oxidation temperature is not related to the chemical composition in a simple manner. It might be expected that the reaction rate will be firstly dependent on the amount of Mn^{2+} ions oxidized and secondly on the nature of the inversion products. This is particularly important with those samples which are not completely oxidized, and there is a higher extent of maganese substitution in which the remaining Mn^{2+} ions form a manganese-rich spinel coexisting with a rhombohedral phase α-$(MnFe)_2O_3$, with rhombohedral α-Fe_2O_3 and with orthorhombic-phase Mn_2O_3.

4. Conclusion

The electrical conductivity data for the $Fe_{3-x}Mn_xO_4$ system are in agreement with the relative availability

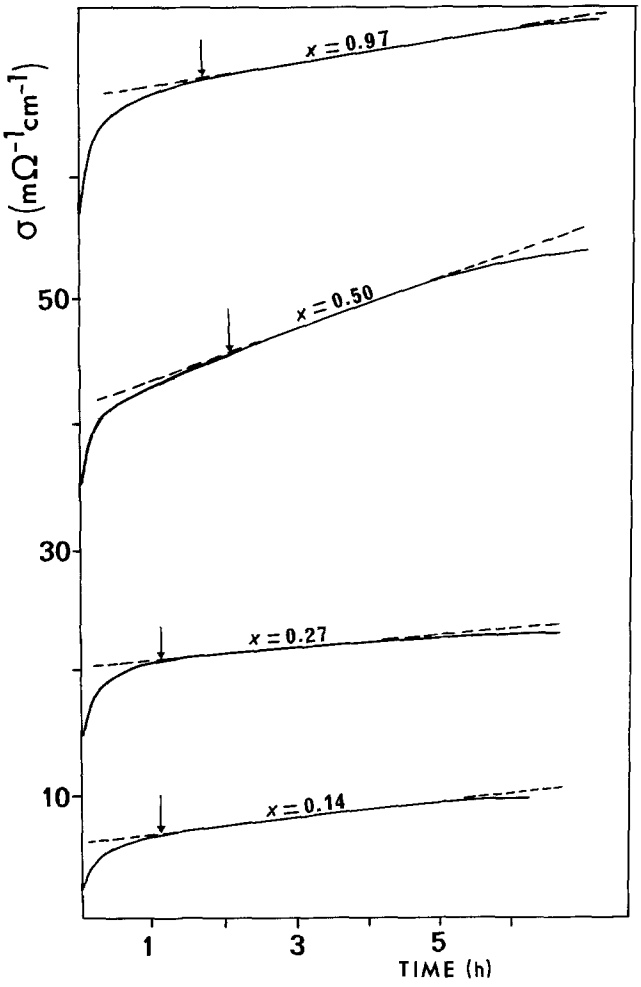

Figure 6 Kinetic curves showing the two steps of oxidation at $P_{O_2} = 2 \times 10^4$ Pa after treatment at low oxygen pressure ($P_{O_2} = 0.3$ Pa). The arrows show the change of kinetic law due to the phase change. $T = 600°$ C.

for oxidation of Fe^{2+} and Mn^{2+} ions, and with the distribution of cations between octahedral and tetrahedral sites in unoxidized substituted magnetites. In the temperature range 150 to 300° C, the Fe^{2+} ions at octahedral sites are oxidized preferentially, producing a large conductivity decrease due to the introduction of vacancies and Fe^{3+} ions at B sites; the electronic exchange between the Fe^{2+} and Fe^{3+} ions is upset. Then, in the temperature range 300 to 400° C, the Mn^{2+} ions at tetrahedral sites are partially oxidized, which favours electron exchange between Mn^{2+} and Mn^{3+} ions present at equivalent sites, here tetrahedral sites. These results are in agreement with the fact that covalent bonding in tetrahedral sites of the spinel structure renders tetrahedral Mn^{2+} ions less available for oxidation than Fe^{2+} ions ionically bound in octahedral sites. When the temperature is raised in the temperature range 400 to 550° C the $\sigma = f(t)$ curves show an increase of conductivity, due probably to the reduction of Mn^{4+} to Mn^{3+} ions with maintenance of the spinel structure. Finally, above 550° C the log $\sigma = f(t)$ curves yield discontinuities attributed to the transformation of a defective spinel into rhombohedral and orthorhombic phases. However, the kinetics of this transformation cannot be directly investigated by following the variation of electrical conductivity in the discontinuity region because of the oxidation of Mn^{2+} ions which accompany the transformation.

References

1. B. GILLOT, F. BOUTON, F. CHASSAGNEUX and A. ROUSSET, *Phys. Status Solidi (a)* **50** (1978) 109.
2. B. GILLOT, R. M. BENLOUCIF and A. ROUSSET, *ibid.* **65** (1981) 205.
3. B. GILLOT, R. M. BENLOUCIF and F. JEMMALI, *J. Mater. Sci.* **19** (1984) 3806.
4. B. GILLOT, F. JEMMALI and A. ROUSSET, *J. Solid State Chem.* **50** (1983) 138.
5. P. TAILHADES, M. EL GUENDOUZI, A. ROUSSET and B. GILLOT, *C.R. Acad. Sci. Paris* **299** Serie II (1984) 13.
6. P. MOLLARD, A. COLOMB, J. DEVENYI, A. ROUSSET and J. PARIS, *IEEE Trans. Mag.* **Mag-11** (1975) 894.
7. J. M. HASTINGS and L. M. CORLISS, *Phys. Rev.* **104** (1956) 328.
8. B. GILLOT and J. F. FERRIOT, *J. Phys. Chem. Solids* **37** (1976) 857.
9. B. GILLOT, D. DELAFOSSE and P. BARRET, *Mater. Res. Bull.* **8** (1973) 1431.
10. B. GILLOT and P. BARRET, *C.R. Acad. Sci. Paris* **278** Serie C (1974) 1477.

Received 26 September
and accepted 14 October 1985